Electrooptical and dynamic properties of 3G cylindrical dendrimers in solutions

Ilya Martchenko,

Department of Physics,
St Petersburg State University, Russia

ilyamartch@mail.ru

University of Fribourg,
Switzerland, Feb. 5, 2009

Introduction: classification of dendrimers

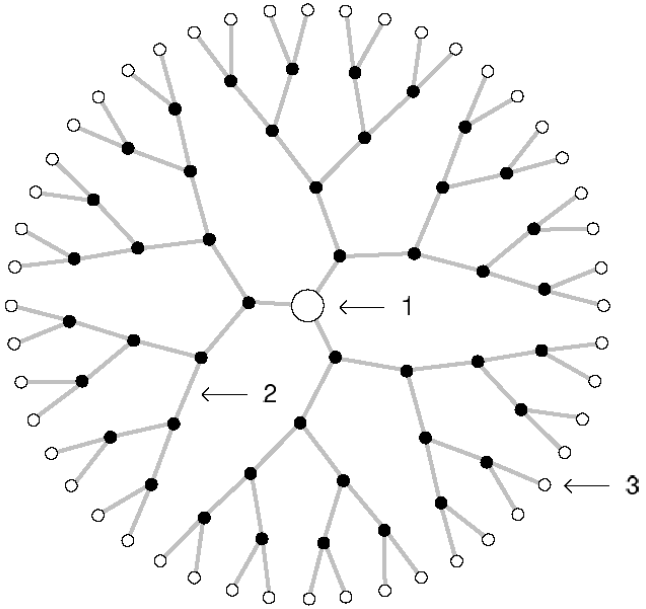

Fig. 1. Spherical dendrimer: core (1), side dendrons (2), terminal groups (3).

- Monodisperse, non-draining particles;
- No dependence of [η] on generation number.

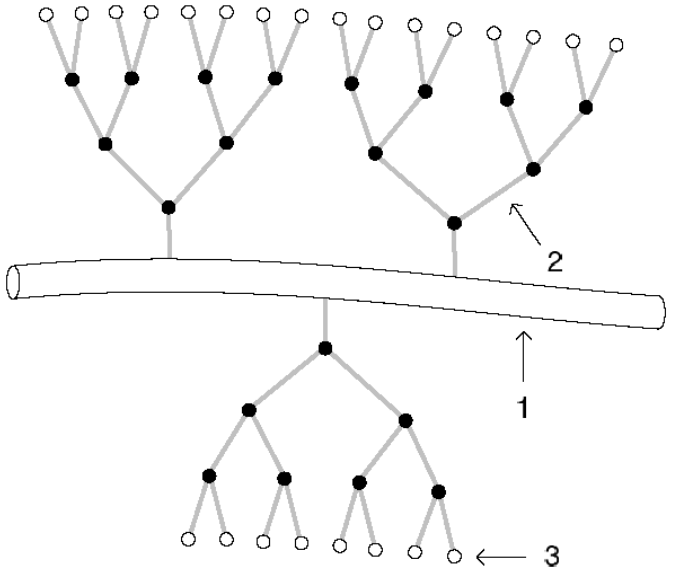

Fig. 2. Cylindrical dendrimer: main polymer chain (1), side dendrons (2), terminal groups (3).

- Anisotropy of properties, a selected axis;
- Equilibrium rigidity typically moderate;
- Properties depend not only on the generation number, but also on the polymerization degree.

Introduction: properties, applications of dendrimers

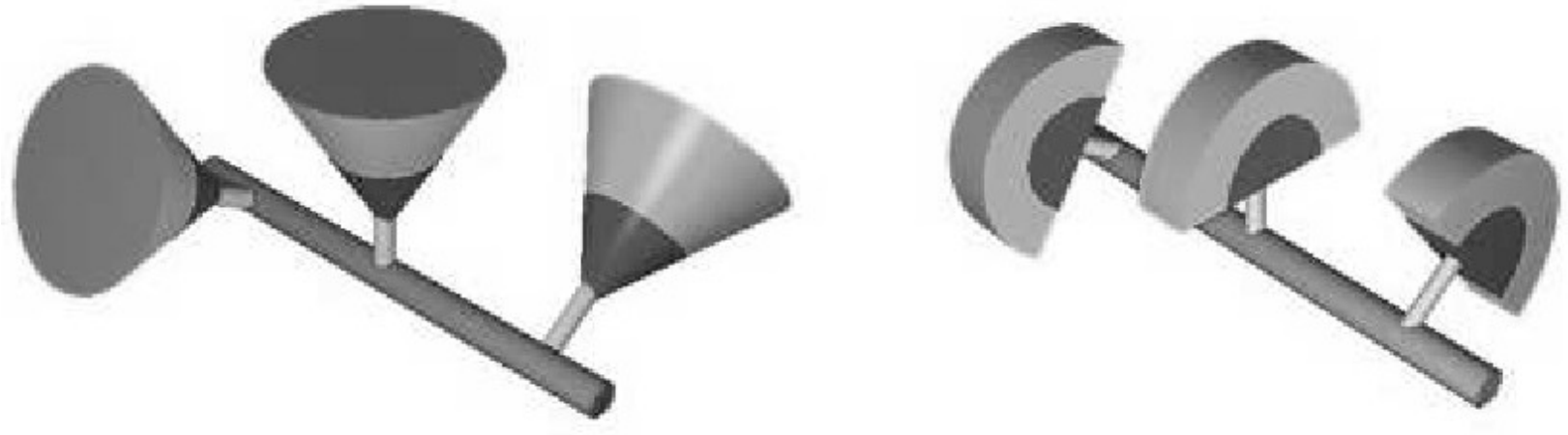

Fig. 3. Scheme of spatial position of dendrons relatively to the main polymer chain.

Sterical interactions between dendritic substituents, their shape, conformation and generation number determine the physical properties of the entire macromolecule.

- Significant interests to dendrimers based on aminoacids
- Drug delivery, pharmaceutics, physiological research

Object of study

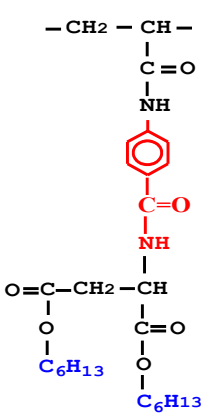

1G

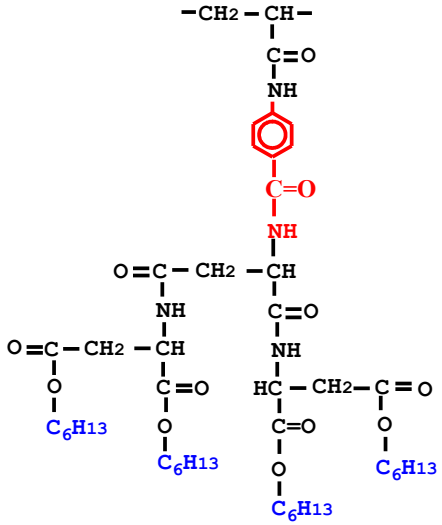

2G

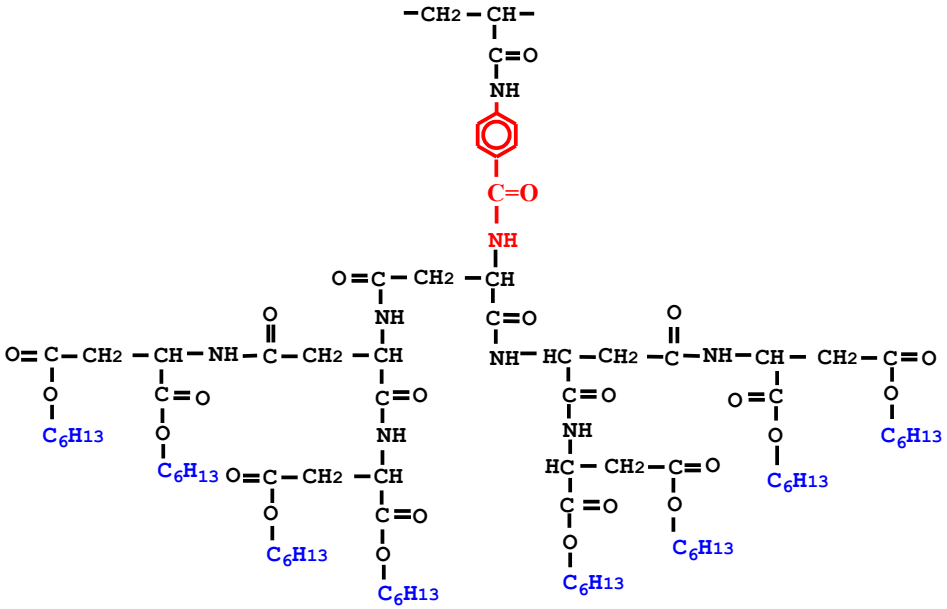

3G

Object of study: 3G samples

- Molecular mass of a monomer unit, $C_{85}O_{24}N_8H_{142}$:

  $M_0 = 1656$ Da.

- Projection of monomer unit on the polymer chain is considered equal to the value for G2:

  $\lambda = 1.53$ Å

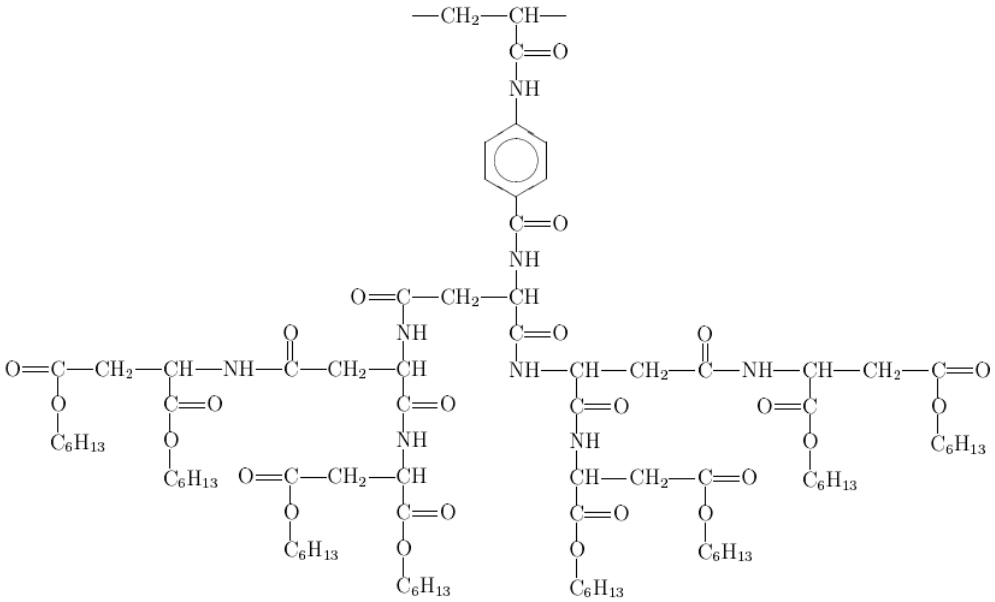

- Eight samples (**“1”**…**“8”**) which vary only in polymerization degree
- Significant number of intermolecular hydrogen bonds between side substituents
- An aromatic anisotropic fragment, increased number of amide groups
- Long terminal aliphatic groups C_6H_{13} increase solubility in organic solvents

Methods

- Isothermal diffusion
- Viscometry
- Sedimentation
- DLS, SLS
- Flow birefringence
- Equilibrium and non-equilibrium electric birefriengence

Theory: Kerr effect

- Kerr constant for solutions:

$$K = \lim_{\substack{c \to 0 \\ E \to 0}} \frac{\Delta n}{cE^2},$$

- Langevin-Borne theory for the dissolved substance with molecules having axial symmetry of optical and dielectic properties:

$$K = \frac{2\pi N_A}{135kT} \frac{(n^2+2)^2}{n} \left(\frac{\varepsilon+2}{3}\right)^2 \frac{\gamma_1 - \gamma_2}{M} \cdot \left(\delta_1 - \delta_2 + \frac{\mu^2}{kT} \frac{3\cos^2\theta - 1}{2}\right),$$

where n is refractive index of solvent, ε is dielectric penetrability of solvent, M is molecular weight of molecule, $(\gamma_1 - \gamma_2)$ is optical anisotropy of molecule, $(\delta_1 - \delta_2)$ is dielectic polarizability of molecule, μ is dipole moment of molecule, θ is angle between the molecule's dipole moment and the symmetry axis of its optical and dielectric polarizabilities, k is Boltzmann constant, N_A is Avogadro number, T is absolute temperature.

- Analysis of equilibrium birefringence provides information on the dipole moment, and also on the conformation of macromolecule.
- Rotational mobility of macromolecules may be studied in a sinusoidal field (non-equilibrium Kerr effect); the Kerr constant at a given frequency is defined as:

$$K_\nu = \frac{\Delta n - \Delta n_0}{cE^2},$$

Methods: Kerr effect

Birefringence was studied in rectangular-pulsed and sinusoidal-pulsed electric fields. Duration of pulses was 3-5 ms at the frequency of 1 pulse per sec. The use of pulsed fields was necessary for eliminating parasite effects not relevant to changes of optical anisotropy (such as heating or ion drift.) A Kerr cell equipped with two titanium electrodes was filled with the studied solution. The gap between the electrodes was equal to d=0,030±0,005 cm, the length of the electrodes along the light path was 3 cm. A solid state laser *HLDPM12-655-5* with wavelength λ=655 nm was used as a light source. In order to improve sensitivity, an
elliptic rotating compensator with the relative path difference of Δλ/λ=0.01 was used.

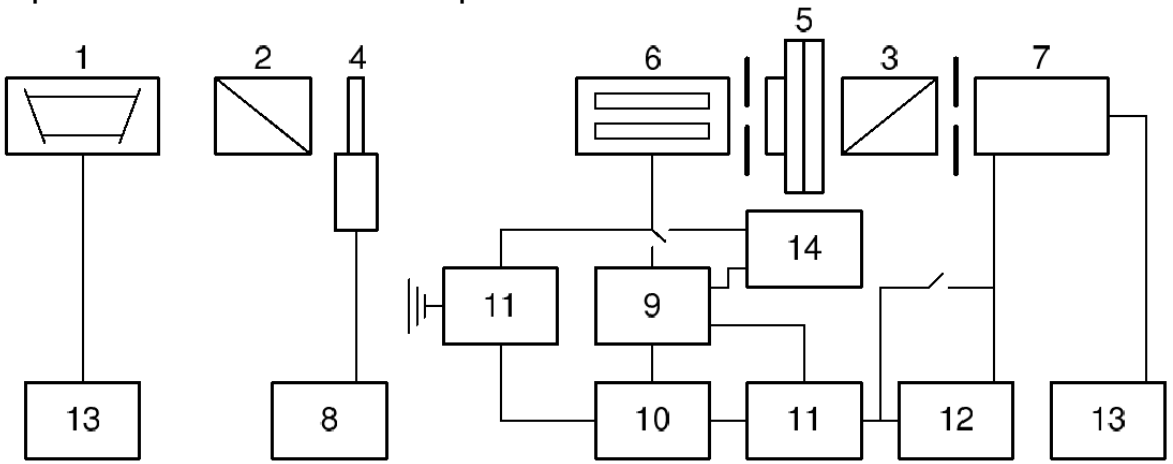

Fig. 5. Scheme of the setup used to measure electric birefringence, solid state laser *HLDPM12-655-5* (1); polarizer (2); analyzer (3); elliptic modulator (4); elliptic compensator (5); Kerr cell with two titanium electrodes (6); photomultiplier (7); generator to excite the oscillations of modulator (8); generator of rectangular pluses (9); pulse generator of delay (10); oscilloscopes (11); selective system (12); power supply units (13), generator of sinusoidal pulses with a multiplier (14).

Methods: flow birefringence

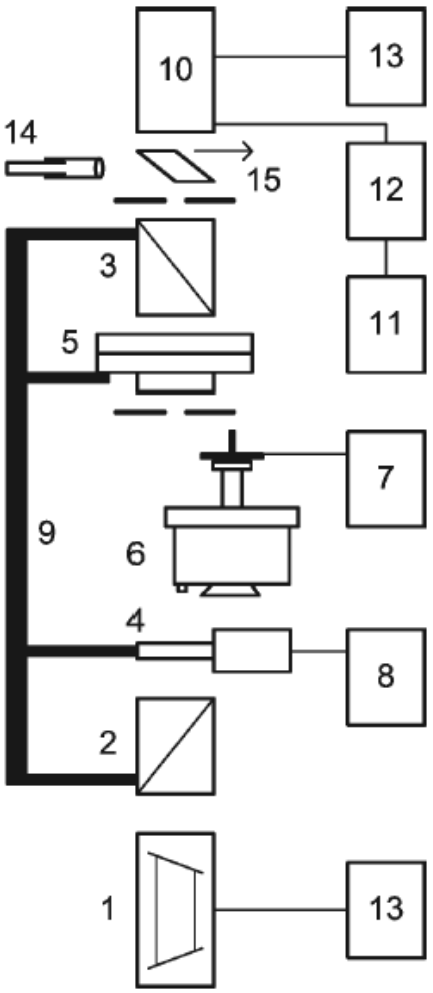

The flow birefringence is a dynamical orientation of non-spherical molecules in a laminar flow. This method permits to directly find the optical anisotropy and rotational diffusion coefficients of macromolecules and helps to effectively study their spatial conformation.

A titanium dynamooptimeter with the height of 3.21 cm and the rotor's diameter of 3 cm. The gap between the concentric cylinders was 0.024 cm. A solid state laser, λ=655 nm. The elliptic rotating compensator had the path difference Δλ/λ=0.035. The measurements were made with a photoelectric sensor. The apparatus was thermostated at 24 °C with water bath. The optical shear coefficient Δn/Δτ is given by:

$$\frac{\Delta n}{\Delta \tau} = \frac{\Delta n_p - \Delta n_0}{g(\eta - \eta_0)},$$

where η is the viscosity of a solution, η_0 is the viscosity of a solvent, Δn_p p is the birefringence of a solution, Δn_0 is the birefringence of a solvent, Δτ is the shear stress, g is the shear rate.

Fig. 6. Scheme of the setup used to measure flow birefringence, solid state laser *HLDPM12-655-5* (1); polarizer (2); analyzer (3); elliptic modulator (4); elliptic compensator (5); dynamooptimeter (6); electric motor (7); generator to excite the oscillations of modulator (8); rotator (9); photomultiplier (10); oscilloscope (11); selective system (12); power supply units (13), ocular (14), mobile prism (15).

Methods: viscometry

Intrinsic viscosities of the polymer solutions have been measured with Ostwald's capillary viscometers with standard methods after long thermostatting at 24 °C.

Efflux time range for used viscometers was 60…90 s.

Results: flow birefringence

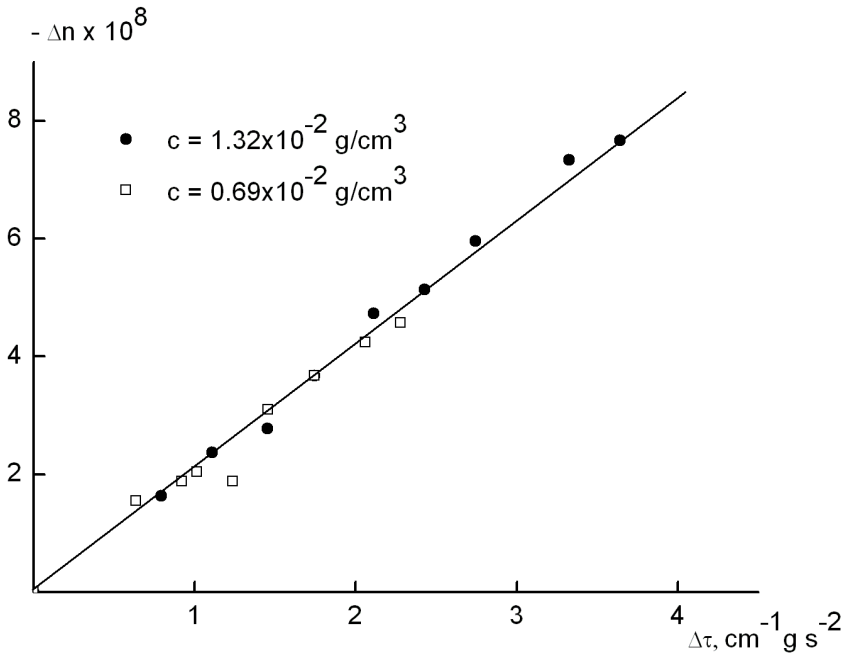

Fig. 22. Dependence of birefringence on the shear stress $\Delta\tau$ for the chloroform solutions of polymer **"7"** at concentrations $c = 1.32 \cdot 10^{-2}$ g/cm^3 (1) and $c = 0.69 \cdot 10^{-2}$ g/cm^3 (2).

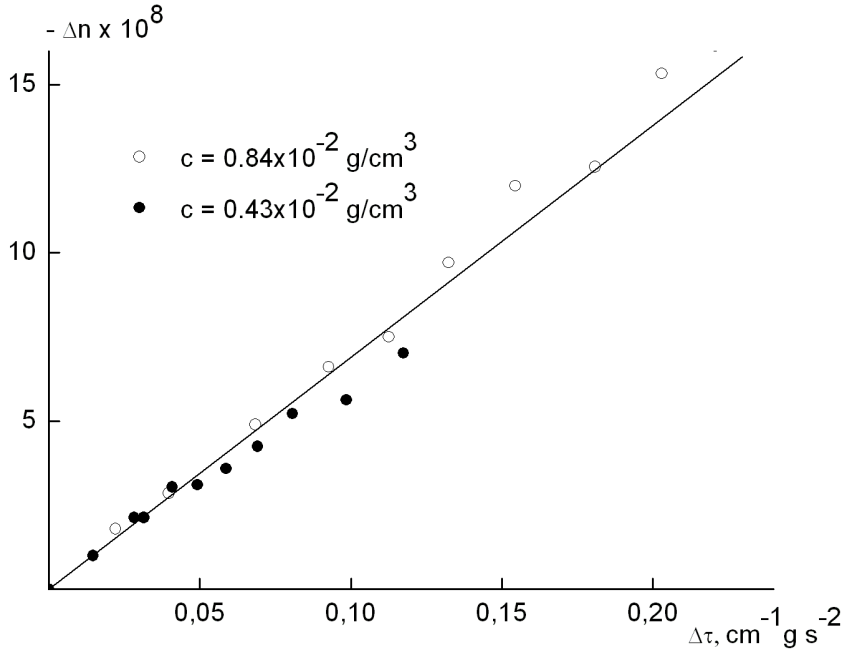

Fig. 24. Dependence of the birefringence on the shear stress $\Delta\tau$ for the dichloroacetic acid solutions of polymer **"4"** at concentrations $c = 0.84 \cdot 10^{-2}$ g/cm^3 (1) and $c = 0.43 \cdot 10^{-2}$ g/cm^3 (2).

- The negative sign of the optical shear coefficient $\Delta n/\Delta\tau$ indicates the negative value of the optical anisotropy Δa of monomer unit of samples in chloroform and DCA.

Discussion: flow birefringence

- Absolute values of flow birefringence constants (*-50…-200×10^{-10} s^{2}cm/g*) for all studied samples exceed the corresponding values for the G1 and G2 samples:
  - 1G dendrimers in bromoform: $\Delta n/\Delta\tau = -50 \cdot 10^{-10}$ *s^{2}cm/g*;
  - 2G dendrimers in bromoform: $\Delta n/\Delta\tau = -25 \cdot 10^{-10}$ *s^{2}cm/g.*

- May be related to increased equilibrium rigidity and increased number of anisotropic groups per unit length of polymer chain.
- With growing generation number, dendrons may be experience more sterical interactions.

Results: equilibrium electric birefringence

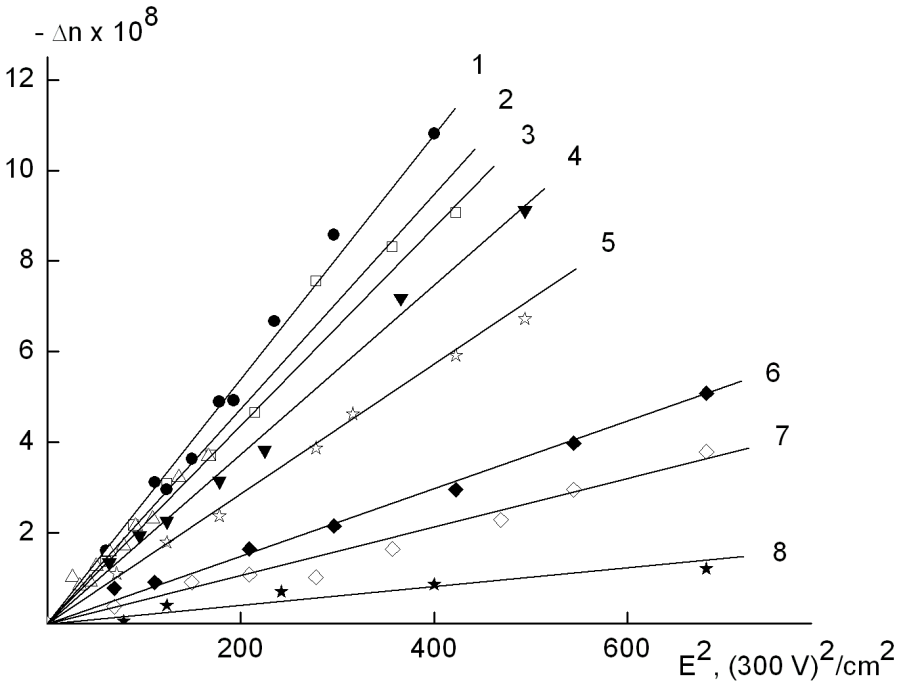

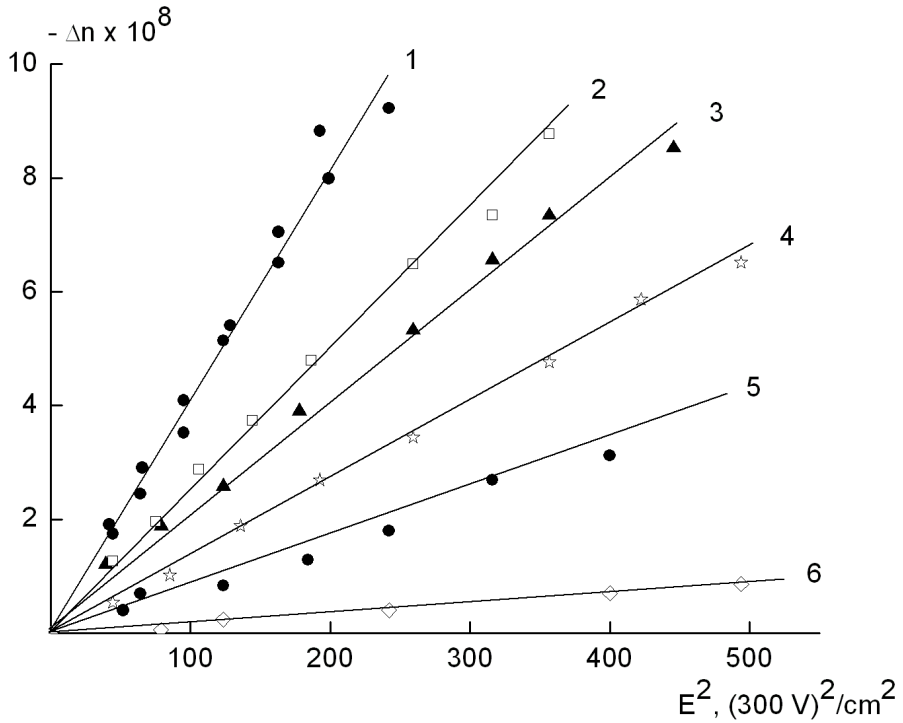

Fig. 7. Dependences of birefringence Δ*n* on the square of rectangular-pulsed electric field E^2 for the chloroform solutions of polymer **"1"** at concentrations $c = 2.88 \cdot 10^{-2}$ g/cm³ (1), $c = 1.67 \cdot 10^{-2}$ g/cm³ (2), $c = 1.10 \cdot 10^{-2}$ g/cm³ (3), $c = 0.75 \cdot 10^{-2}$ g/cm³ (4), $c = 0.52 \cdot 10^{-2}$ g/cm³ (5), $c = 0.17 \cdot 10^{-2}$ g/cm³ (6), $c = 0.09 \cdot 10^{-2}$ g/cm³ (7), and data of pure chloroform (8).

Fig. 8. Dependences of birefringence Δ*n* on the square of rectangular-pulsed electric field E^2 for the chloroform solutions of polymer **"7"** at concentrations $c = 1.32 \cdot 10^{-2}$ g/cm³ (1), $c = 0.69 \cdot 10^{-2}$ g/cm³ (2), $c = 0.43 \cdot 10^{-2}$ g/cm³ (3), $c = 0.23 \cdot 10^{-2}$ g/cm³ (4), $c = 0.12 \cdot 10^{-2}$ g/cm³ (5), and data of pure chloroform (8).

Results: concentration dependence of Kerr constant

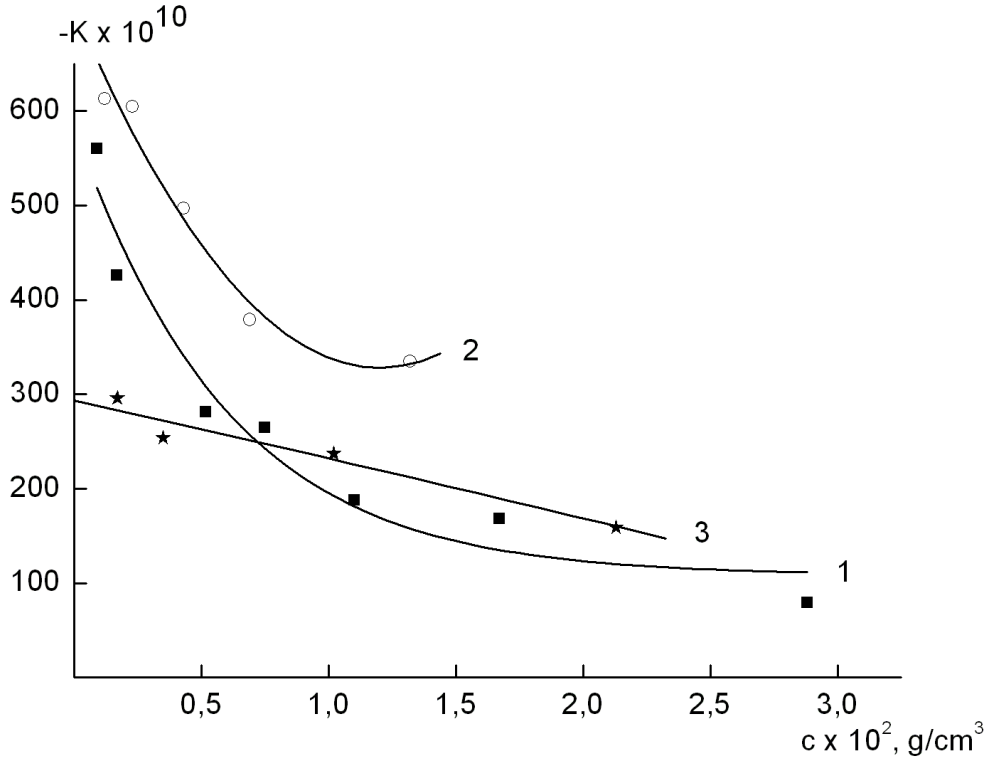

Fig. 9. Dependence of Kerr constants on the concentration of polymers **“1”** (1), **“6”** (2), **“7”** (3).

- The absolute values of Kerr constants increase as a solution is diluted. Similar behavior: aromatic polyamides solved in dimethylamide and dimethylsulphoxide.
- The growth is most likely caused by charge effects and the change of dielectric properties of solutions at dilution. Worth noting that chloroform is a much less polar and less conducting solvent than dimethylamide and dimethylsulphoxide.

Results: non-equilibrium electric birefringence

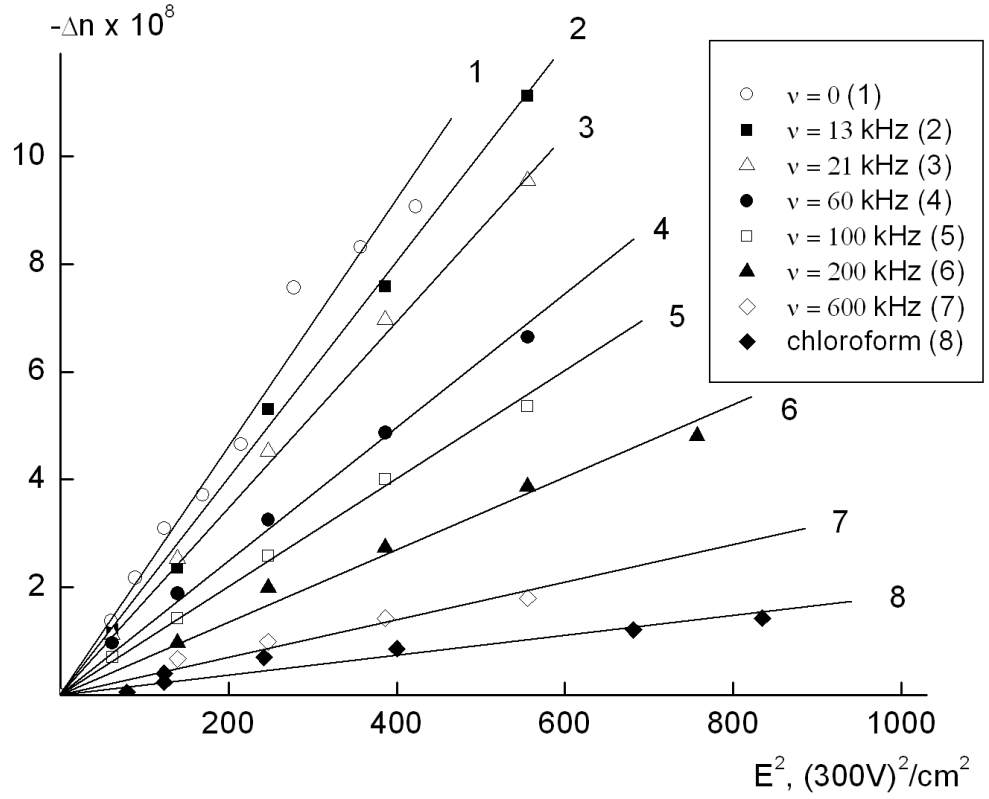

Fig. 10. Dependences of birefringence Δ*n* on the square of sinusoidal-pulsed electric field E^2 for the chloroform solution of polymer **"1"** at the concentration $c = 2.88 \cdot 10^{-2}$ *g/cm*^{3}. The plot includes data for the frequencies *0 Hz* (1), *13 kHz* (2), *21 kHz* (3), *60 kHz* (4), *100 kHz* (5), *200 kHz* (6), *600 kHz* (7), and data of pure chloroform (8).

- In the studied strength range, the plots are straight lines obeying the Kerr law
- Electric birefringence demonstrate dispersion

Results: non-equilibrium electric birefringence

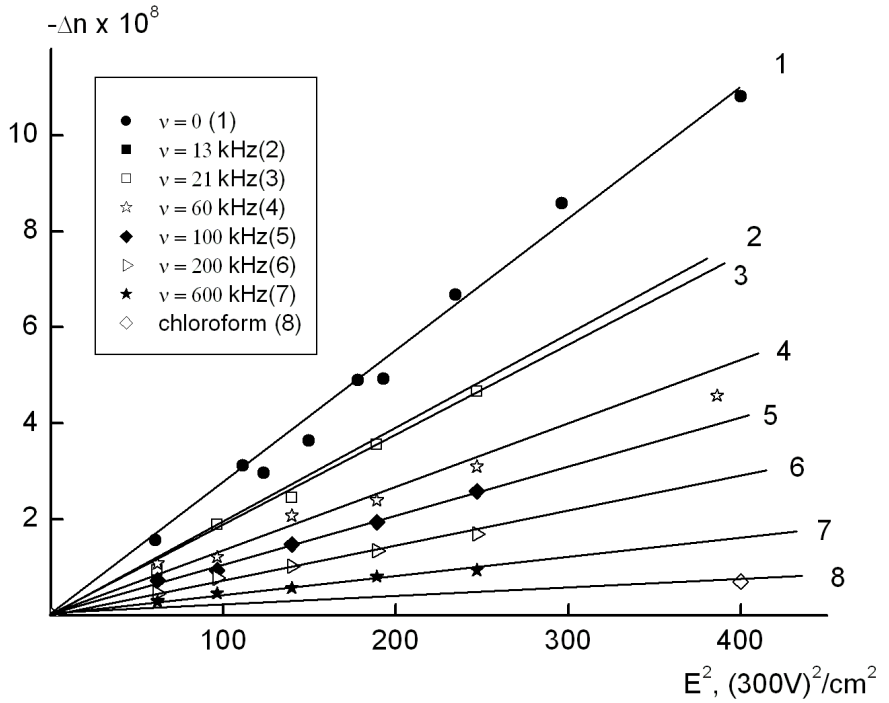

Fig. 11. Dependences of birefringence Δ*n* on the square of sinusoidal-pulsed electric field E^2 for the chloroform solution of polymer **"1"** at the concentration $c = 1.67 \cdot 10^{-2}$ *g/cm³*. The plot includes data for the frequencies *0 Hz* (1), *13 kHz* (2), *21 kHz* (3), *60 kHz* (4), *100 kHz* (5), *200 kHz* (6), *600 kHz* (7), and data of pure chloroform (8).

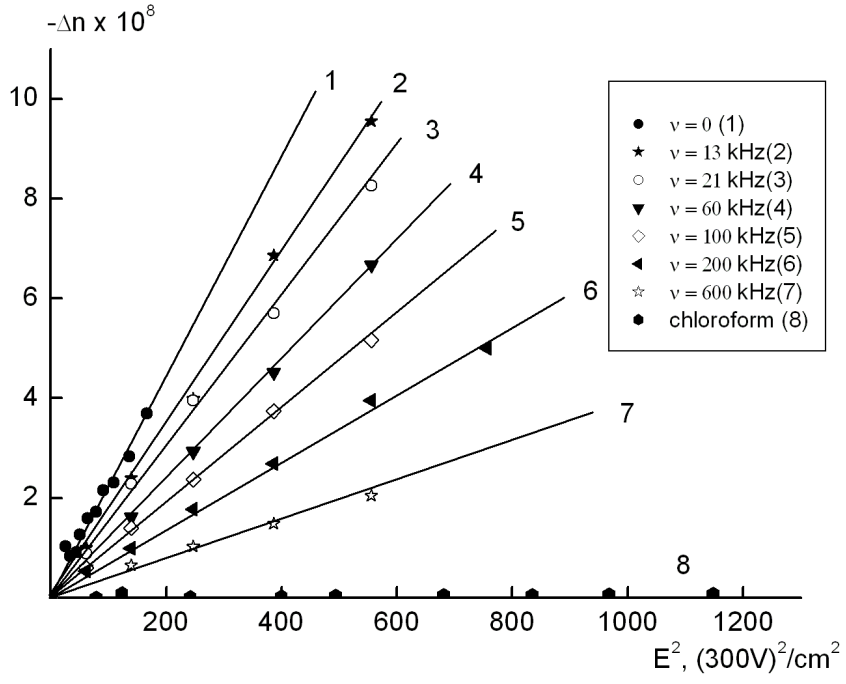

Fig. 12. Dependences of birefringence Δ*n* on the square of sinusoidal-pulsed electric field E^2 for the chloroform solution of polymer **"1"** at the concentration $c = 1.10 \cdot 10^{-2}$ *g/cm³*. The plot includes data for the frequencies *0 Hz* (1), *13 kHz* (2), *21 kHz* (3), *60 kHz* (4), *100 kHz* (5), *200 kHz* (6), *600 kHz* (7), and data of pure chloroform (8).

Results: non-equilibrium electric birefringence

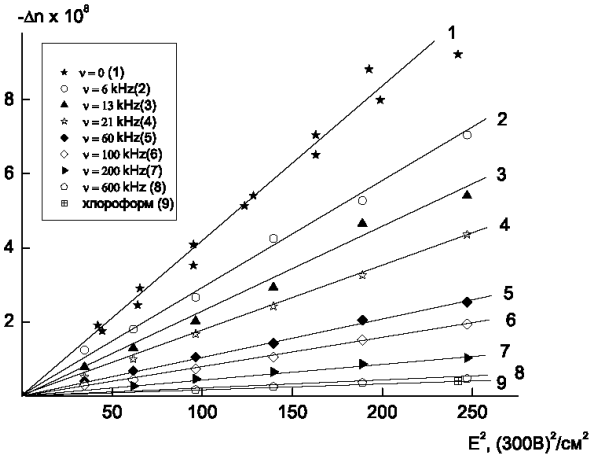

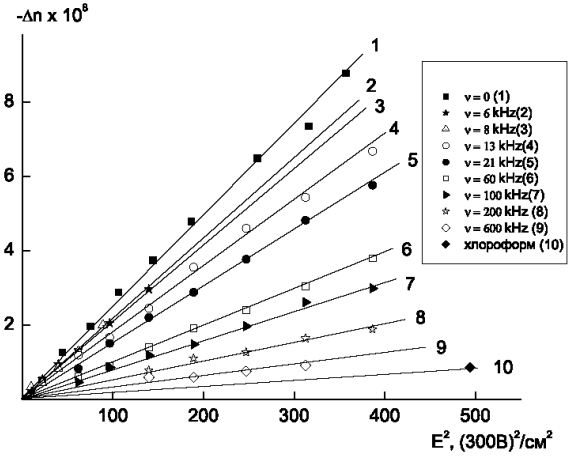

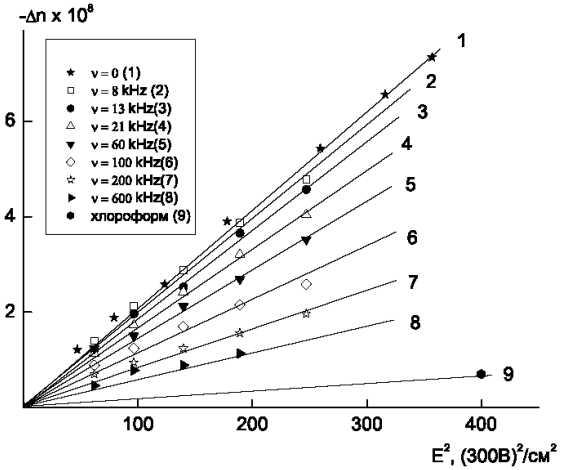

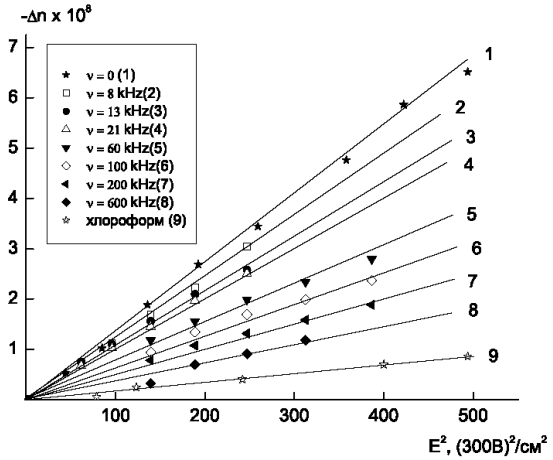

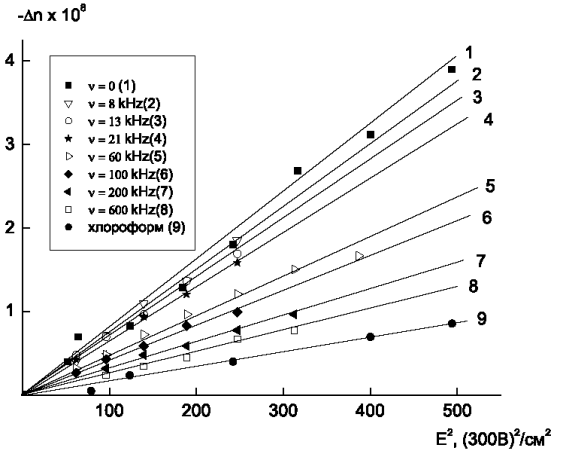

Fig. 13, 14, 15, 16, 17. Dependences of birefringence Δn on the square of sinusoidal-pulsed electric field E^2 for the chloroform solutions of polymer **"7"** at frequencies in the range 0…600 kHz and at concentrations $c = 1.32 \cdot 10^{-2}$ *g/cm³* (**13**), $c = 0.69 \cdot 10^{-2}$ *g/cm³* (**14**), $c = 0.43 \cdot 10^{-2}$ *g/cm³* (**15**), $c = 0.23 \cdot 10^{-2}$ *g/cm³* (**16**), $c = 0.12 \cdot 10^{-2}$ *g/cm³* (**16**).

Results: dispersion of Kerr effect

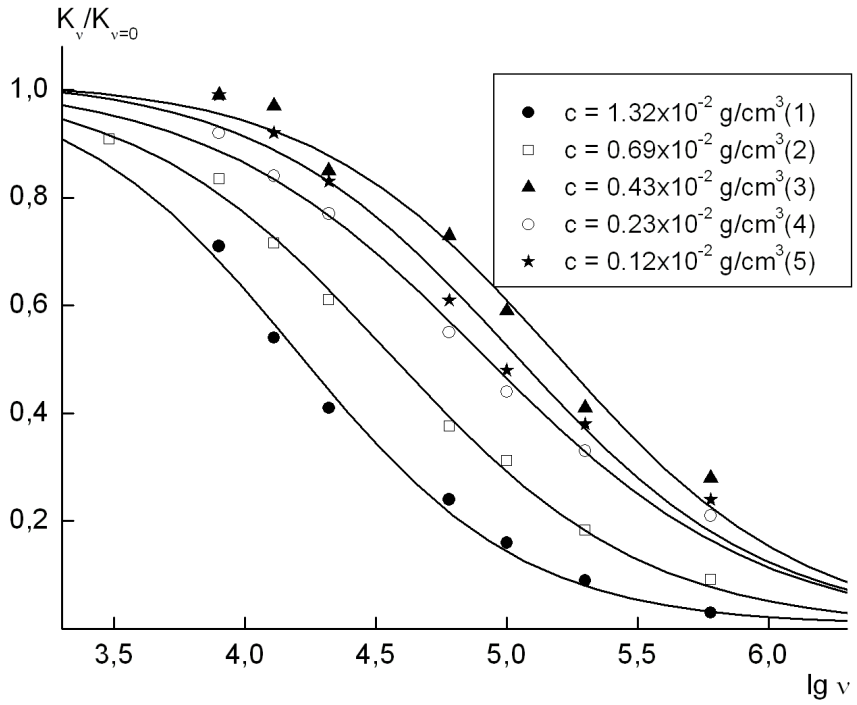

Fig. 18. Dispersion curves of specific Kerr constant $K_\nu/K_{\nu\to 0}$ for the chloroform solutions of polymer **"7"** at concentrations $c = 1.32\cdot10^{-2}$ *g/cm³* (1), $c = 0.69\cdot10^{-2}$ *g/cm³* (2), $c = 0.43\cdot10^{-2}$ *g/cm³* (3), $c = 0.23\cdot10^{-2}$ *g/cm³* (4), $c = 0.12\cdot10^{-2}$ *g/cm³* (5).

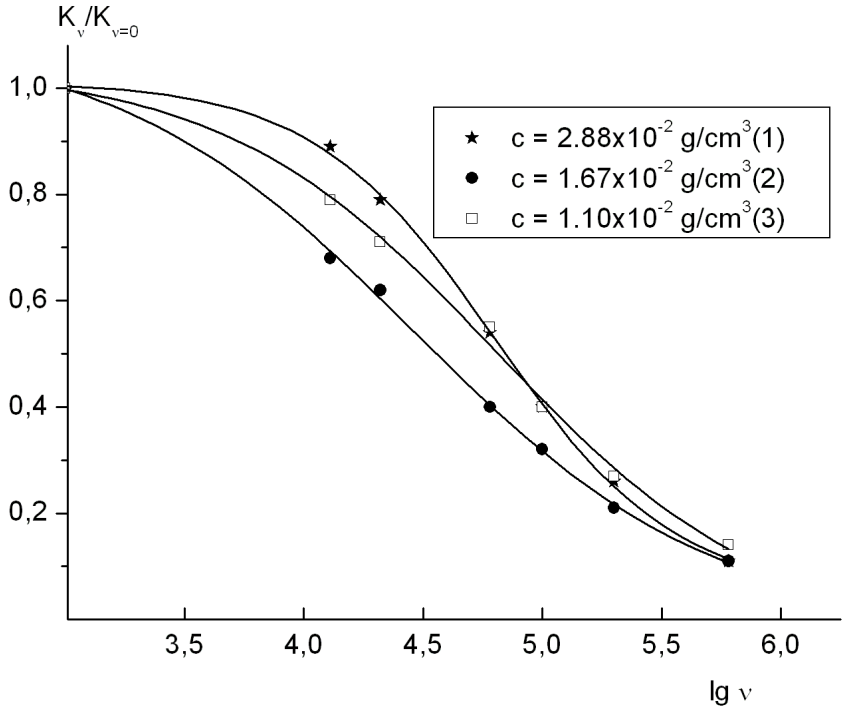

Fig. 19. Dispersion curves of specific Kerr constant $K_\nu/K_{\nu\to 0}$ for the chloroform solutions of polymer **"1"** at concentrations $c = 2.88\cdot10^{-2}$ *g/cm³* (1), $c = 1.67\cdot10^{-2}$ *g/cm³* (2), $c = 1.10\cdot10^{-2}$ *g/cm³* (3).

Results: dispersion of Kerr effect

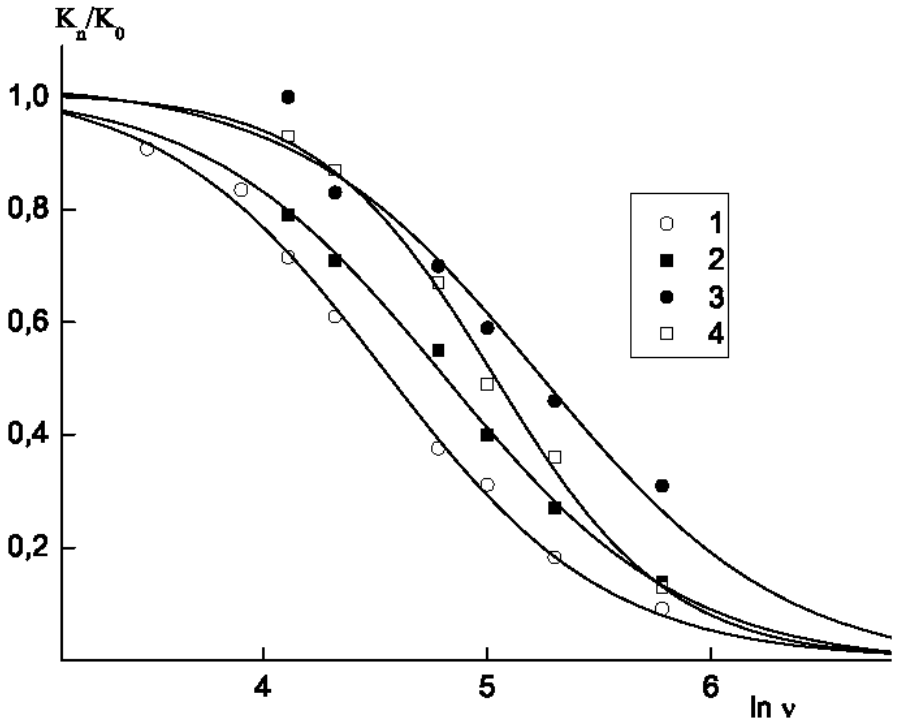

Рис. 20. Dispersion curves of specific Kerr constant $K_v/K_{v\to 0}$ for the chloroform solutions of polymers **“7”** (1), **“1”** (2), **“5”** (3), **“4”** (4) at the least studied concentrations.

- Dispersion dependences of the samples decay virtually to zero
- Macromolecules undergo the reorientation in external fields with the dipole mechanism

What happens when intermolecular hydrogen bonds are broken?

- Dichloroacetic acid can be used for degradation of hydrogen bonds

Results: non-equilibrium birefringence in DCA

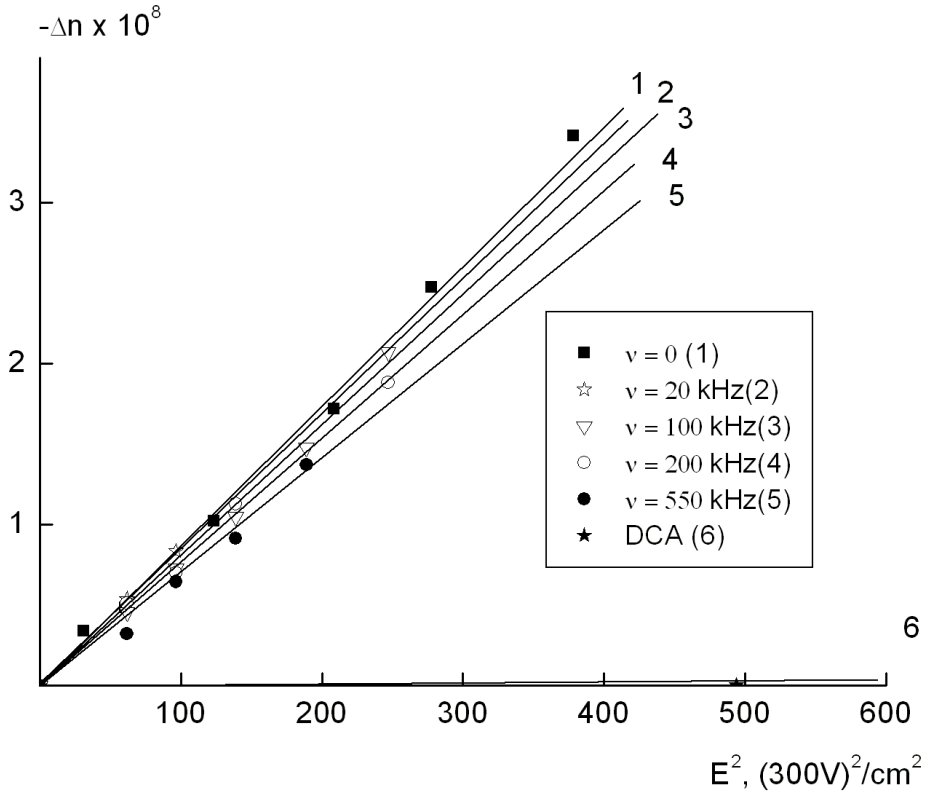

Fig. 21. Dependences of birefringence Δn on the square of sinusoidal-pulsed electric field E^2 for the DCA solution of polymer **"4"** at the concentration $c = 0{,}84 \cdot 10^{-2}$ *g/cm*^{3}. The plot includes data for the frequencies *0 Hz* (1), *20 kHz* (2), *100 kHz* (3), *200 kHz* (4), *550 kHz* (5), and data of pure DCA (6).

- The magnitude of electric birefringence decays with growing frequency *v* of sinusoidal-pulsed field.
- However, the birefringence does not approach the half its equilibrium values at the frequencies below *1 Mhz* (maximum possible value for the experimental equipment)
- Absolute values of Kerr constants in DCA as smaller than in chloroform.

Theory: non-equilibrium electric birefringence

- Kerr constant at a given frequency:

$$K_\nu = \frac{\Delta n - \Delta n_0}{cE^2},$$

- The mean dispersion relaxation times $\tau = 1/(2D_r)$, where D_r is the rotational coefficient of diffusion relative to the short axis of a macromolecule, may be found with the expression:

$$\tau = \frac{1}{\omega_m}.$$

- where $\omega_m = 2\pi\nu_m$ is the frequency that corresponds to the half-decay of the electric birefringence dispersion effect:

$$K_{\nu_m} = \frac{K_{\nu=0} - K_{\nu\to\infty}}{2},$$

Dynamic properties of macromolecules

- Relaxation times $\tau = 1/(2D_r)$, molar masses M and intrinsic viscosity $[\eta]$ have a relation expressed by:

$$M[\eta]\eta_0 D_r = FRT,$$

- where D_r is rotational diffusion coefficient with respect to short axis of a molecule, F is model parameter that characterizes the dimensions and the conformation of a, R is gas constant, T is absolute temperature.

- For rigid particles the values of *F* range from 0.13 for a rod to 0.42 for a spherical particle.

- For **solutions in chloroform** ($\eta_0 = 0{,}547 \cdot 10^{-2}$ *P*) *F* were found in the range **0,01…0,11**
  - reveals a large scale mechanism of reorientation, corresponds to a rigid rod.
- For **solutions in DCA** ($\eta_0 = 7 \cdot 10^{-2}$ *P*), the upper limit of relaxation times and the lower limit of *F* were found through Debye extrapolation:***3…6***
  - seriously exceeds the maximum theoretically possible value 0.42 for kinetically rigid molecules
- In DCA, macromolecules undergo reorientation according to low scale mechanism
- Explained by degradation of intermolecular hydrogen bonds and growth of kinetic rigidity of chains

V.N. Tsvetkov. *Zhestkotsepnye polimernye molekuly* (Nauka, 1986), p. 335, 339

Discussion: Kerr effect

- Absolute values of Kerr constants ($-100\ldots-300\times10^{-10}$ $g^{-1}cm^5(300\ V)^{-2}$) for all studied samples exceed the corresponding values for the G1 and G2 samples:
  - 1G dendrimers in bromoform: $K = -150\cdot10^{-10}$ $g^{-1}cm^5(300\ V)^{-2}$;
  - 2G dendrimers in bromoform: $K = -60\cdot10^{-10}$ $g^{-1}cm^5(300\ V)^{-2}$.
- The growth may be related to increased number of anisotropic groups per unit length of polymer chain.
- Similar (negative) signs of K and $\Delta n/\Delta\tau$ are explained by similar (large scale) reorientation mechanism in hydrodynamic and electric fields.
- Observation that the Kerr constants in DCA solutions are smaller than in chloroform may be related to decreasing optical anisotropy of monomer unit Δa (evident through flow birefringence).

What do we know about spatial conformation and shape of studied 3G dendrimers?

- Translational coefficients of diffusion
- Contour length of polymer chains

Shape of macromolecules: analysis

№	M	$D \cdot 10^7$, cm^2/s
"1"	76500	7.3
"2"	60300	7.5
"3"	59000	8.0
"4"	58600	8.5
"5"	48200	8.8
"6"	32500	9.7
"7"	30500	10.0
"8"	19000	12.6

№	$L \cdot 10^8$, cm	$f \cdot 10^8$, erg·s/cm^2
"1"	72.3	5.67
"2"	57.0	5.52
"3"	55.8	5.18
"4"	55.4	4.87
"5"	45.6	4.70
"6"	30.7	4.27
"7"	28.4	4.14
"8"	18.0	3.29

Chain length:

$$L = \frac{M\lambda}{M_0}$$

Einstein formula:

$$f = \frac{kT}{D}$$

Translational coefficients of diffusion are found with methods of isothermal diffusion and sedimentation by S.V. Bushin's group (Inst. of Macromol. Compounds, Russian Acad. Sci.) and with DLS by S.K. Filippov (Prague)

N.V. Tsvetkov, L.N. Andreeva, S.K. Filippov, S.V. Bushin, M.A. Bezrukova, I.A. Martchenko, I.A. Strelina, V.P. Alyabyeva, N.V. Girbasova, A.Yu. Bilibin. Polymer Sci. A (to appear in 2009)

Shape of macromolecules: analysis

- Fujita's theory for spherocylinders:

$$f = \frac{3\pi\eta_0 L}{\ln L/d + Q\,(d/L)},$$

- where *Q (d/L)* is power law:

$$Q\left(\frac{d}{L}\right) = 0{,}3863 + 0{,}6863\left(\frac{d}{L}\right) - 0{,}06250\left(\frac{d}{L}\right)^2 - 0{,}01042\left(\frac{d}{L}\right)^3 - \\ - 0{,}000651\left(\frac{d}{L}\right)^4 + 0{,}0005859\left(\frac{d}{L}\right)^5 + \cdots$$

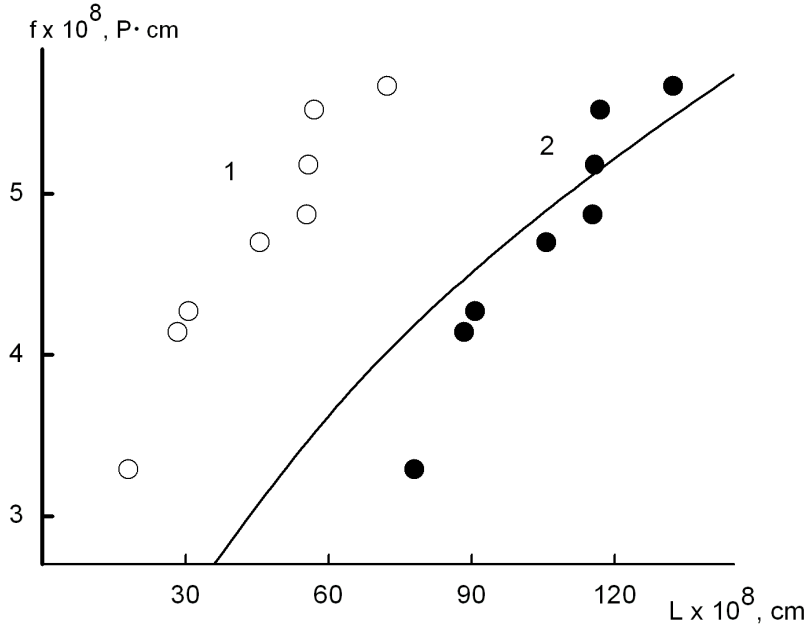

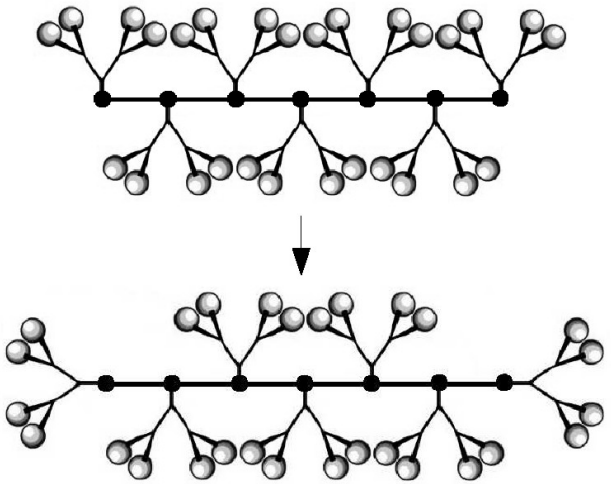

1 is the length of the main polymer chain itself;
2 is the same data increased with *ΔL= 60 Å*

T. Norisuye, M. Motowoka and H. Fujita. Macromolecules, **12**, No. 2, 320-323 (1979)

Properties of studies samples

№	$[\eta]$, dL/g	$D_d \cdot 10^7$, cm^2/s	$D_{DLC} \cdot 10^7$, cm^2/s	M_W	M_{SD}	$M_{D\eta}$	N	$\Delta n/\Delta\tau \cdot 10^{10}$, s^2cm/g	$K \cdot 10^{10}$, $g^{-1}\ cm^5\ (300\ V)^{-2}$	$\tau \cdot 10^6$, s	F
Chloroform solutions											
"1"	0.16	7.3			76500		46	−170	−(170 . . .560)	2.4	0.06
"2"	–		7.5 ± 0.3	60300			36				
"3"	0.14	8				59000	36	−165	−(250 . . .330)	0.8	0.11
"4"	0.12	8.5				58600	35	−220	−(210 . . .270)	1.2	0.06
"5"	0.12		8.8 ± 0.2	48200		51000	30				
"6"	0.14	9.7				32500	20	−205	−(160 . . .295)	6	0.01
"7"	0.14	10	8.3 ± 0.3	30500		30000	18	−170	−(185 . . .260)	1.2	0.04
"8"	0.11	12.6				19000	11	−150	−(170 . . .560)	2	0.01
Dichloroacetic acid solutions											
"3"	0.08					59000	36	−70	−(90 . . .115)	<0.2	>3.3
"4"	0.08					58600	35	−65	−(105 . . .125)	<0.1	>6.5
"7"	0.10			30500			18	−68			

Conclusions

- **1.** Absolute values of Kerr and Maxwell constants are found to exceed the corresponding values for the dendrimers of lower generations. 3G samples have a considerably larger negative optical anisotropy of a monomer unit than the 1G and 2G polymers of the same series.
- **2.** It is shown that the studied macromolecules with polymerization degrees 10…40 have small asymmetry of shape.
- **3.** Results from hydrodynamic methods indicate that the terminal side dendrons are oriented mainly along the primary molecular chain, which is confirmed by the methods of flow birefringence and electric birefringence.
- **4.** The structure of side dendrons and the generation number determine the conformational, optical and dipole characteristics of macromolecular cylindrical dendrimers.
- **5.** It is found that the reorientation mechanism is determined by physical and chemical properties of solvent.
- **6.** Intermolecular hydrogen bonds in the studied third-generation cylindrical dendrimers provide high kinetic rigidity. The degradation of hydrogen bonds in dichloroacetic acid leads to a sharp drop in kinetic rigidity of macromolecules.

References

[1] P.J. Flory. J. Amer. Chem. Soc., **74**, 2718-2723 (1952)

[2] *Dendrimers*. Ed. by F. Vögtle (Springer-Verlag, 1998)

[3] D.A. Tomalia et al. Polym. J. (Tokyo), **17**, 117-132 (1985)

[4] G.R. Newkome et al. J. Org. Chem., **50**, No. 11, 2003-2004 (1985)

[5] A.M. Muzafarov et al. Uspekhi Khimii, 60, No. 7, 1596-1612 (1991)

[6] M. Freemantle. Chemistry and Engineering News, 27-35 (Nov. 1, 1999)

[7] V. Percec et al. J. Chem. Amer. Soc., **120**, 43, 11061-11070 (1998)

[8] J.-P. Majoral et al. Chem. Commun., 2929-2942 (2002)

[9] B. Mandelbrot. *Les objets fractals, survol du langage fractal* (Flammarion, 1975)

[10] B. Klajnert et al. Acta Biochemica Polonica, **48**, 1, 198-208 (2001)

[11] D.K. Smith et al. Top. Curr. Chem., **210**, 183-227 (2000)

[12] K. Sugiura. Top. Curr. Chem., **228**, 65–85 (2003)

[13] N. Ouali et al. Macromolecules, **33**, 6185-6193 (2000)

[14] A.V. Lezov et al. Polymer Sci. A, **48**, No. 3, 325-331 (2006)

[15] I. Neubert et al. Macromol. Chem. Phys., **17**, 517-527 (1996)

[16] Liquid Crystal Dendrimers group, the University of Sheffield, 2005, at *http://www.shef.ac.uk/materials/liquid_crystal/dend/*

[17] C.C. Lee et al. Macromolecules, **39**, No. 2, 476-481 (2006)

[18] A. Lubbert et al. Macromolecules, **38**, No. 6, 2064-2071 (2005)

[19] L. Harnau et al. J. Chem. Phys., **127**, 014901-014906 (2007). arXiv: 0705.3331v1

[20] P.-G. de Gennes. Croatica Chemica Acta, **71**, 4, 833-836 (1998)

[21] M. Mondeshki et al. Macromolecules, **39**, No. 26, 9605-9613 (2006)

[22] S. Langereis et al. Eindhoven Univ. of Tech., 2001, retrieved at *http://www.bmt.tue.nl/research/pdf/postersonderzoekdag2001/slangereis.pdf*

[23] R.M. Crooks et al. Acc. Chem. Research, **34**, 3, 181-190 (2001)

[24] Цитата по: Berkeley Lab Research Review (2001)

[25] S.V. Bushin et al. Polymer Sci. A, **44**, No. 6, 632-639 (2002)

[26] N.V. Tsvetkov et al. Polymer Sci. A, **45**, No. 2, 145-148 (2003)

[27] N.V. Girbasova et al. Polymer Sci. A, **45**, No. 4, 550-561 (2003)

[28] S.V. Bushin et al. Polymer Sci. A, **47**, No. 2, 175-182 (2005)

[29] L.N. Andreeva et al. Polymer Sci. A, **47**, No. 8, 875-884 (2005)

[30] N.V. Tsvetkov et al. Polymer Sci. A, **48**, No. 5, 520-526 (2006)

[31] A.Yu. Bilibin et al. Polymer Sci. A, **49**, No. 4, 363-372 (2007)

[32] S.V. Bushin et al. Polymer Sci. A, **49**, No. 7, 843-850 (2007)

[33] N.V. Tsvetkov et al. Polymer Sci. A, **50**, No. 2, 119-128 (2008)

[34] S.V. Bushin , N.V. Tsvetkov, I.A. Martchenko et al. Proc. 6th International Symposium *Molecular Order and Mobility in Polymer Systems* (St Petersburg, Russia, June 6-8, 2008), p. 98

[35] N.V. Tsvetkov, L.N. Andreeva, S.K. Filippov, S.V. Bushin, M.A. Bezrukova, I.A. Martchenko, I.A. Strelina, V.P. Alyabyeva, N.V. Girbasova, A.Yu. Bilibin. Polymer Sci. A (to appear in 2009)

[36] I. Martchenko, N. Tsvetkov. Trudy MFTI (to appear in 2009) arXiv:0809.3907v1 [cond-mat.soft]

[37] I.A. Martchenko. Abstr. *Physics and Progress* (St Petersburg State University, Oct. 25-27, 2006), p. 184-186

[38] N.V. Tsevtkov, L.N. Andreeva, I.A. Strelina, T.A. Dmitrieva, I.A. Martchenko et al. Proc. 4th Kargin Conference (Moscow State University, Jan. 29-Feb. 2, 2007), Vol. 3, p. 65

[39] I.A. Martchenko, N.V. Tsvetkov. Abstr. 3rd Conf. *Modern Problems of Polymer Science* (Institute of Macromolecular Compounds, Russian Academy of Sciences, St Petersburg, Russia, April 17-19, 2007), p. 220

[40] I.A. Martchenko. Abstr. Conf. *Physics and Progress* (St Petersburg State University, Nov. 14-16, 2007), p. 306-310

[41] I.A. Martchenko, N.V. Tsvetkov. Proc. 50th MIPhT Conf. (Moscow, Nov. 23-26, 2007), p. 98-99

[42] N.V. Tsvetkov, I.A. Martchenko et al. Proc. 4th Conf. *Modern Problems of Polymer Science* (Inst. of Macromol. Compounds, Russian Acad. Sci., April 15-17, 2008), p. 2-P-68

[43] I. Martchenko. Abstr. Conf. *Physics and Progress* (St Petersburg State University, Nov. 19-21, 2008), p. 111

[44] R.K. Sinnott. *Coulson & Richardson's Chemical Engineering, Vol. 6* (Butterworth-Heinemann, 4th ed, 1999), p. 473

[45] V.N. Tsvetkov. *Zhestkotsepnye polimernye molekuly* (Nauka, 1986), p. 335, 339

[46] T. Norisuye, M. Motowoka and H. Fujita. Macromolecules, **12**, No. 2, 320-323 (1979)

[47] V.N. Tsvetkov. *Zhestkotsepnye polimernye molekuly* (Nauka, 1986), p. 39–40

Properties of studies samples: index

- Intrinsic viscosities $[\eta]$;
- Translational coefficients of diffusion D_d obtained from isothermal diffusometry;
- Translational coefficients of diffusion D_{DLS} obtained from DLS;
- Molecular masses M_W found from partition functions of relaxation times, in DLS;
- Molecular mass M_{SD} calculated for sample **"1"** in chloroform with the data for D_d and the flotation factor s measured on the unltracentrifuge;
- Molecular masses $M_{D\eta}$ found from experimental values of D and $[\eta]$;
- Polymerization degrees N;
- Maxwell constants (optical shear coefficients) $\Delta n/\Delta\tau$;
- Kerr constants K;
- Average rotational relaxation times τ;
- Model parameters F.